

Analysis of sports related mTBI injuries caused by elastic wave propagation through brain tissue

David Case and Edmond Richer*

Biomedical Instrumentation and Robotics Laboratory,
Southern Methodist University

ABSTRACT

Repetitive concussions and sub-concussions suffered by athletes have been linked to a series of sequelae ranging from traumatic encephalopathy to dementia pugilistica. A detailed finite element model of the human head was developed based on standard libraries of medical imaging. The model includes realistic material properties for the brain tissue, bone, soft tissue, and CSF, as well as the structure and properties of a protective helmet. Various impact scenarios were studied, with a focus on the strains/stresses and pressure gradients and concentrations created in the brain tissue due to propagation of waves produced by the impact through the complex internal structure of the human head. This approach has the potential to expand our understanding of the mechanism of brain injury, and to better assess the risk of delayed neurological disorders for tens of thousands of young athletes throughout the world.

1. INTRODUCTION

In recent years, mild traumatic brain injury (mTBI) has received more and more attention due to the large number of high school, college, and professional athletes affected during sporting events. Repetitive concussions and sub-concussions have been linked to a series of sequelae ranging from traumatic encephalopathy to dementia pugilistica [1–3].

It has been documented that brain injuries occur not only in areas adjacent to the skull, as predicted by the coup/counter-coup models, but also at relatively great depths within the brain tissue. This suggests a more subtle injury mechanism, not based on direct contact deformation under external stresses.

Numerous researchers focused on linear and angular accelerations of the head and the associated effects on brain tissue deformation (see [1, 3–5] and references therein). They used reconstruction of impacts from game videos or accelerometer-based telemetry systems as input data, derived brain tissue stress/strain distribution from sophisticated finite element (FE) computer models, and validated their models on mannequins or cadavers in order to assess the risk of injury [3, 4, 6, 7]. These studies suggest that transient gradients of the stresses/strains within the brain tissue are the root cause of later neurological dysfunctions.

While a lot of attention has been given to the brain injury due to direct contact phenomena and to the effect of linear and angular accelerations of the head during an impact, very few studies have examined the effect of wave propagation through the brain tissue [8–10]. Moreover, none of these studies were conducted in the context of sports-specific injuries.

*Corresponding Author: E-mail: richer@smu.edu

2. FINITE ELEMENT MODELING

2.1 MODELING BASED ON MR IMAGES AND SEGMENTATION

Our work is aimed to improve the existing FE models used to predict the effect of impact on the brain, by taking into consideration the strains/stresses and pressure gradients created in the brain tissue by the propagation of elastic waves produced by the impact. Due to the complex internal structure of the human head, containing tissues with intricate anatomy and vastly different mechanical properties (from bone to cerebral spinal fluid (CSF)), multiple reflections, refractions, interferences, and resonant phenomena are expected. These in turn have the potential to create sharp moving pressure and strain gradients as well as areas of stress concentration that will increase the risk of brain tissue damage and the probability of future neurological sequelae.

To test the feasibility of the proposed approach we built a detailed model of the helmet/head system based on standard medical Magnetic Resonance (MR) brain images. Without loss of generality, a two-dimensional model was assembled, based on the CT scan of a human adult from the front of the head, focused at the midbrain (Fig. 1a). Image segmentation was used to differentiate between brain structures, skull, various types of soft tissue, and the CSF. The primary bony structures seen in this cross-section are the parietal and temporal plates of the skull and the mandible. Between the bony protrusions of the mandible are the soft tissues of the throat, tongue, and pallet. Finally, the brain itself is shown, with apparent lateral and third ventricles, surrounded by cerebral fluid. Encasing the skull is a thin layer of soft tissue, representing the skin (Fig. 1b). The FE model was augmented with a protective helmet represented by a configuration of foam rubber pads and impact plastic in direct contact with the skin. The entire assembly was surrounded by an air environment. As shown in Table 1, the model includes realistic material properties of the brain as well as the other head tissues: bone, soft tissue, skin, and CSF [3, 11]. The protective helmet padding was modeled as foam rubber and the shell as impact plastic.

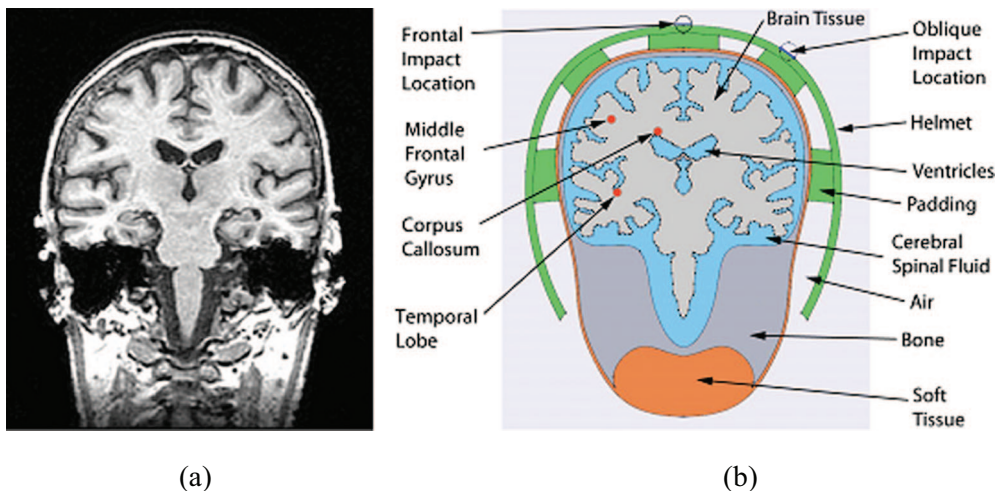


Figure 1: Modeling based on anatomical MR images of a human head focused on the midbrain (a) and tissue identification based on image segmentation (b). Points of particular interest for measurement are indicated in red (from top to bottom: middle frontal gyrus, corpus callosum, and temporal lobe at the lateral sulcus)

Table 1: Material properties for biological tissues and protective helmet

Material	Density ρ [kg/m ³]	Speed of Sound c [m/s]
Air	1,1225	340
Bone	2,100	3,200
CSF	1,040	1,433
Soft Tissue	1,000	1,540
Foam Rubber	1,190	60
Impact Plastic	1,190	2,870

2.2 SIMULATION PHYSICS

The Acoustic-Solid Interaction Module of COMSOL Multiphysics (COMSOL Inc., Burlington, MA) was used for time-dependent FE analysis. The solid domains were modeled as linear elastic material, subject to

$$\rho \frac{\partial^2 \mathbf{u}}{\partial t^2} - \nabla \cdot \boldsymbol{\sigma} = \mathbf{F} \quad (1)$$

where \mathbf{u} is a displacement vector, \mathbf{F} represents any external strains or loads, and the scalar $\boldsymbol{\sigma}$ term is the double dot product of the strain tensor and a Rayleigh damping matrix, derived as follows:

$$\boldsymbol{\sigma} = \mathbf{C}_R : (\boldsymbol{\varepsilon}) \equiv \sum_i \sum_j \mathbf{C}_{Rij} \varepsilon_{ji} \quad (2)$$

$$\mathbf{C}_R = \alpha_{dM} \mathbf{m} + \beta_{dk} \mathbf{k} + \mathbf{C} \quad (3)$$

where \mathbf{m} and \mathbf{k} are the mass and stiffness matrices of the material, respectively, and $\alpha_{dM} = 1/80 \text{ s}^{-1}$ and $\beta_{dk} = 0.0003 \text{ s}$ are the associated damping parameters. The remaining “weak static” contribution, \mathbf{C} , is the elasticity tensor derived from the associated material’s Young’s modulus and Poisson’s ratio.

For the fluid domain a time-varying pressure field was modeled based on the following wave equation:

$$\frac{1}{\rho c^2} \frac{\partial^2 p}{\partial t^2} + \nabla \cdot \left(-\frac{1}{\rho} (\nabla p - \mathbf{q}) \right) = Q \quad (4)$$

Here, ρ and c represent the density and speed of sound within the local material, p represents the local pressure, and \mathbf{q} and Q represent any present dipole or monopole source terms, respectively.

The boundary condition defined between the solid and fluid domains is as follows:

$$\boldsymbol{\sigma} \cdot \mathbf{n} = p \mathbf{n} \quad (5)$$

$$-\mathbf{n} \cdot \left(-\frac{1}{\rho} (\nabla p - \mathbf{q}) \right) = -\mathbf{n} \cdot \mathbf{u} \quad (6)$$

where \mathbf{n} is the outward pointing unit normal vector, as seen from inside the solid domain. These equations define the fluid loads on the solid domain and the structural acceleration’s effect on the fluid.

In the assembled model, a monopole source term is placed at the outer surface of the helmet, above the second foam pad on the right-hand side for oblique impact analysis and directly above the third pad for frontal impact analysis. These represent two possible impact scenarios during the sporting activity. The source is given a Gaussian time profile,

$$Q = -A 2\pi^2 f^2 (t - t_p) e^{-\pi^2 f^2 (t - t_p)^2} \quad t_p - 1/f < t < t_p + 1/f \quad (7)$$

with amplitude $A = 1 \text{ m}^2/\text{s}$, frequency bandwidth $f = 100\text{Hz}$, f and pulse peak time $t_p = 0.01\text{s}$. The outer limits of the surrounding air domain are given a “plane wave –radiation” boundary condition to allow outgoing waves to leave the modeling domain without reflection:

$$-\mathbf{n} \cdot \left(-\frac{1}{\rho} (\nabla p - \mathbf{q}) \right) + \frac{1}{\rho} \left(\frac{1}{c} \frac{\partial p}{\partial t} \right) = Q \quad (8)$$

2.3 MESHING

The FE mesh for oblique impact analysis is shown in Fig. 2 and consisted of 56,794 triangular elements, with size adjusted automatically according to the complexity of the anatomical features. The mesh for frontal impact analysis was comparable, consisting of 56,896 triangular elements. The relevant statistics and parameters for both models are as follows: Minimum Element Quality – 0.3552; Average Element Quality – 0.9323; Maximum Growth Rate – 2.755 (oblique)/3.064 (frontal); Average Growth Rate – 1.406.

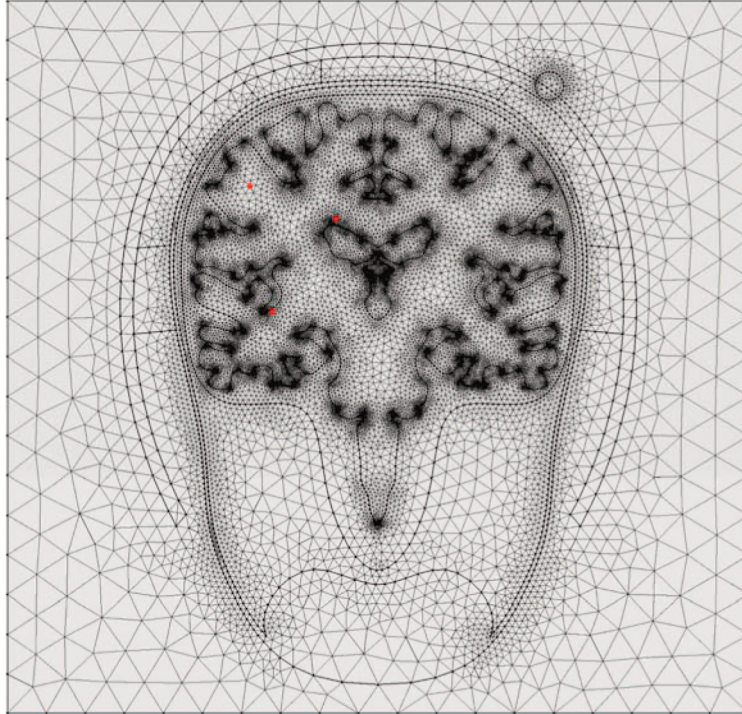


Figure 2: Finite element mesh consisting of 56,794 triangular elements

3. SIMULATION RESULTS AND ANALYSIS

A Dell OptiPlex 7010 work station with 3rd Gen Intel Quad Core i5-3470, and 16 GB DDR3, 1600 MHz RAM was used to run the time-dependent *Multifrontal Massively Parallel sparse direct Solver* (MUMPS). The time interval was set for 100 ms after impact, with 0.1 ms steps, and a scaled absolute tolerance of 0.001. A *Fully Coupled* node that uses a damped version of Newton's method was employed with *Termination technique* set to a *Tolerance factor* = 1.

The results of the time-dependent analysis for the oblique impact scenario are shown in Fig. 3. Post-processing reveals the propagation of the acoustic wave (with sound level in dB) through the helmet and head. The results for the air domain are not shown to increase the clarity of the results in the areas of interest. As expected, the initial wave rapidly progresses through the helmet and head. Due to the small wave attenuation through the CSF and brain tissue [11], the wave is reflected and refracted multiple times at the interfaces between the inner surface of the skull, auditory system, and internal brain structures. Sharp gradients and pressure foci develop in the temporal lobes, frontal Gyri, and corpus callosum starting 15 ms after impact and lasting for approximately 50 ms (see Fig. 3c – 3h). In some of these areas the absolute pressure can even exceed the maximum value at the impact site, as seen in Fig. 4. Furthermore, these maximum values are dependent upon the location of the impact site. A peak impact pressure value of 1,000 Pa at an oblique angle on the surface of the helmet produces a 2,700 Pa peak value in the temporal lobe with an oblique impact scenario and a 3,500 Pa peak value with a frontal impact scenario (Fig. 5).

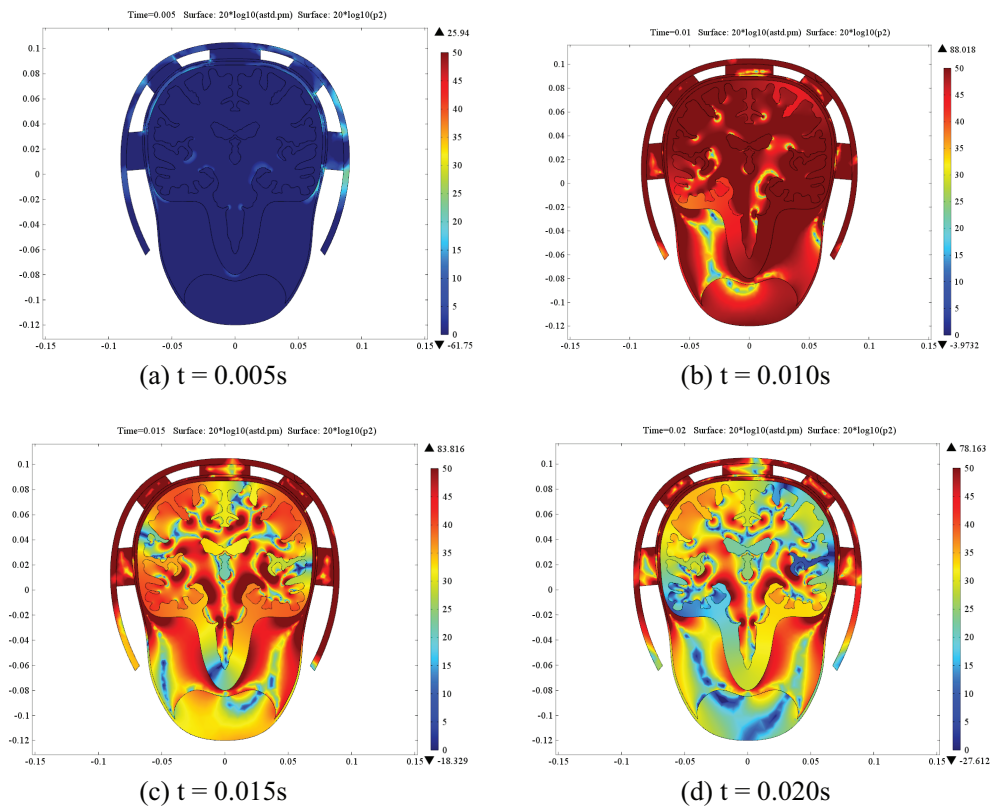


Figure 3: (Continued)

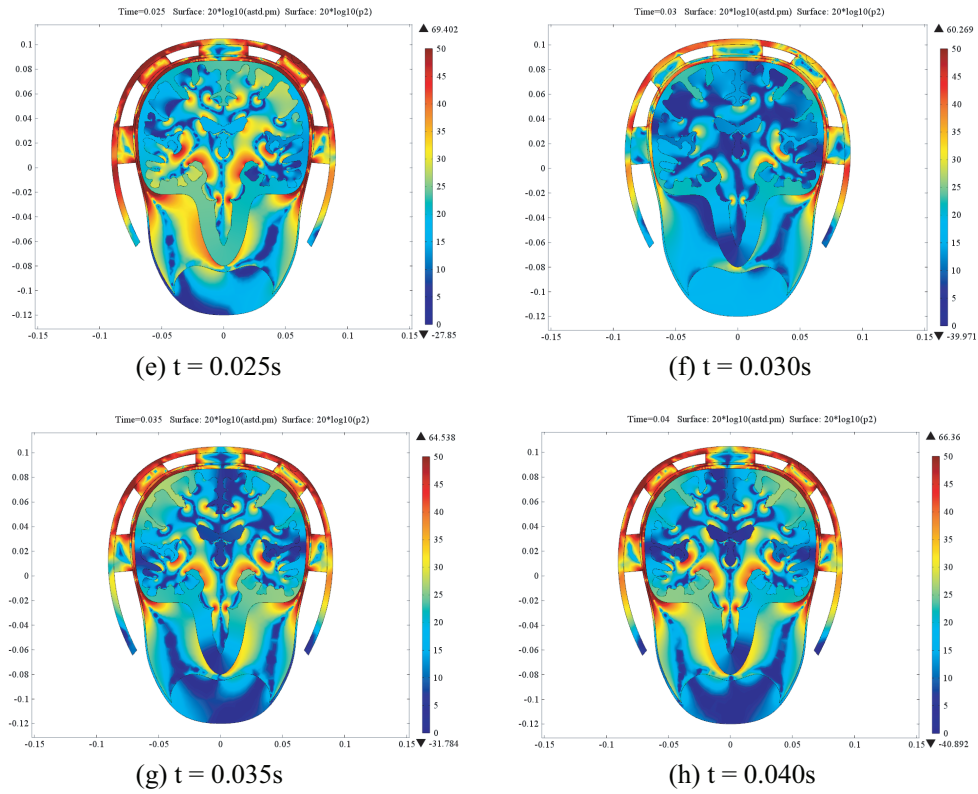


Figure 3: Time series ($t = 0 - 40$) of finite element simulation results showing the sound level in decibels

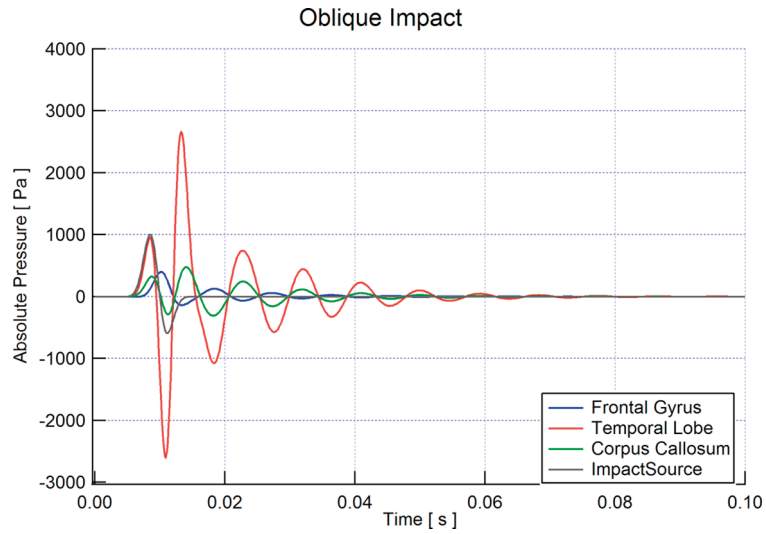


Figure 4: Absolute pressure foci in selected areas of the brain in reaction to an oblique impact

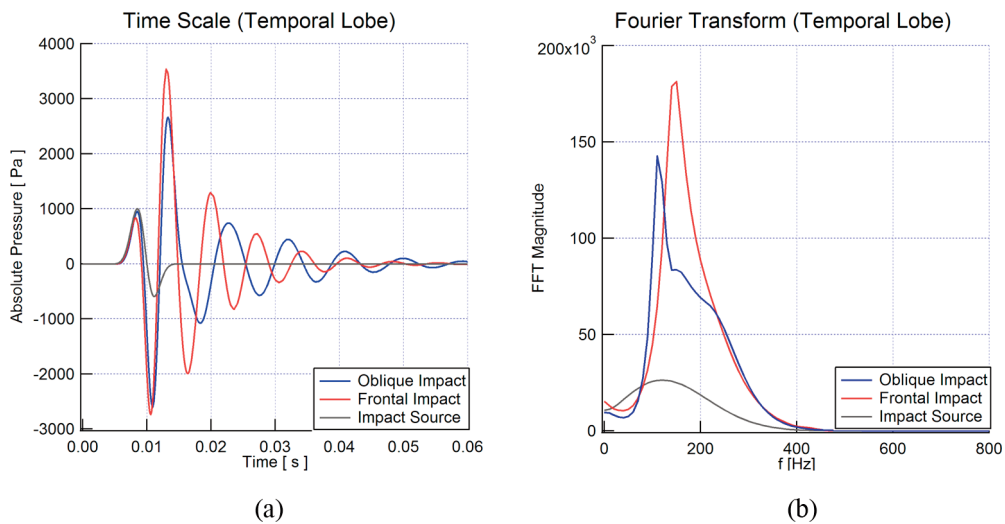


Figure 5: Comparison of pressure focus in the temporal lobe under oblique and frontal impact scenarios. Pressure focus is shown on a time scale (a) and with frequency composition (b)

4. CONCLUSIONS

We developed a detailed FE model of an athlete's head based on standard libraries of medical imaging. The model includes realistic material properties of the brain tissue, bone, soft tissue, and CSF, as well as a protective helmet. The results show that foci of intense pressure concentration are formed in specific areas of the brain, possibly exceeding the maximum pressure applied to the helmet surface. These pressure foci are dependent upon the location of impact and have the potential of inducing significant strains and stresses that would supplement the ones predicted by acceleration-based analysis.

The detailed time domain FE analysis of the pressure wave propagation through the athlete's head has the potential to expand our understanding of the mechanism of brain injury and improve the accuracy of mTBI prediction. Moreover, it opens the ability to create personalized models of mTBI based on MR images of individual players and real time game impact data. This can lead to better assessment of risk of injury and of delayed neurological disorders for tens of thousands of young athletes throughout the world.

REFERENCES

- [1] Dashnaw, M., Petraglia, A. and Bailes, J., 2012. "An overview of the basic science of concussion and subconcussion: where we are and where we are going". *Neurosurgical Focus*, 33, pp. 1–9.
- [2] Kelly, J., Amerson, E. and Barth, J., 2012. "Mild traumatic brain injury: Lessons learned from clinical, sports, and combat concussions". *Rehabilitation Research and Practice*, 2012, pp. 1–5.
- [3] Viano, D., Casson, I., Pellman, E., Zhang, L., King, A. and Yang, K., 2005. "Concussion in professional football: Brain responses by finite element analysis: Part 9". *Neurosurgery*, 57, pp. 891–915.

- [4] Funk, J., Rowson, S., Daniel, R. and Duma, S., 2012. "Validation of concussion risk curves for collegiate football players derived from HITS data". *Annals of Biomedical Engineering*, 40, pp. 79–89.
- [5] Meaney, D. and Smith, D., 2011. "Biomechanics of concussion". *Clinical Sports Medicine*, 30, pp. 19–31.
- [6] Willinger, R., Kang, H.-S. and Diaw, B., 1999. "Three-dimensional human head finite-element model validation against two experimental impacts". *Annals of Biomedical Engineering*, 27, pp. 403–410.
- [7] Schatz, P. and Zillmer, E., 2003. "Computer-based assessment of sports-related concussion". *Applied Neuropsychology*, 10, pp. 42–47.
- [8] Clayton, E., Genin, G. and Bayly, P., 2010. "Wave propagation in the human brain and skull imaged in vivo by MR elastography". In *Proceedings of the International Federation for Medical and Biological Engineering*.
- [9] Yin, X. and Hynynen, K., 2005. "A numerical study of transcranial focused ultrasound beam propagation at low frequency". *Physics in Medicine and Biology*, 50, pp. 1821–1836.
- [10] Shahsavari, S., McKlevey, T., Ritzen, C. and Rydenhag, B., 2011. "Cerebrovascular mechanical properties and slow waves of intracranial pressure in TBI patients". *IEEE Transactions on Biomedical Engineering*, 58, pp. 2072–2082.
- [11] Kremkau, F., Barnes, R. and McGraw, C., 1981. "Ultrasonic attenuation and propagation speed in normal human brain". *The Journal of the Acoustical Society of America*, 70, pp. 29–38.